Journal of Applied and Computational Mechanics, Vol. 3, No. 2, (2017), 125-134
DOI: 10.22055/JACM.2017.21581.1109

Journal of
Applied and Computational Mechanics

Electromechanical Performance of NEMS Actuator Fabricated from Nanowire under quantum vacuum fluctuations using GDQ and MVIM

Fateme Abadian[1,*], Rahman Soroush[2], Alireza Yekrangi[3]

[1] Department of Mathematics, Isfahan (Khorasgan) Branch, Islamic Azad University
Isfahan, Iran, abadian.naeini@yahoo.com
[2] Department of Engineering, Lahijan Branch, Islamic Azad University
Lahijan, Iran, eng.soroush322@yahoo.com
[3] Department of Engineering, Ramsar Branch, Islamic Azad University
Ramsar, Iran, yekrangi_ali@yahoo.com

Received March 23 2017; revised May 24 2017; accepted for publication May 31 2017.
Corresponding author: Fateme Abadian, abadian.naeini@yahoo.com

Abstract

The Casimir attraction can significantly interfere with the physical response of nanoactuators. The intensity of the Casimir force depends on the geometries of interacting bodies. The present paper is conducted to model the influence of the Casimir attraction on the electrostatic stability of nanoactuators made of the cylindrical conductive nanowire/nanotube. An asymptotic solution, based on the path-integral approach, is employed to investigate the Casimir force. Moreover, the continuum theory is employed to derive the constitutive equation of the actuator. On the other hand, the governing nonlinear equations are solved by three different approaches, and also various perspectives of the issue including comparison with the van der Waals (vdW) force regime, the variation of instability parameters and the effect of geometry are addressed.

Keywords: Casimir attraction, Continuum model, Electromechanical stability, Generalized Differential Quadrature (GDQ), Modified Variation Iteration Method (MVIM).

1. Introduction

Relying on recent developments in nanotechnology, engineers have become able to fabricate nanoscale electromechanical systems (NEMS) which are beneficial in electronics, biology, etc. These miniature systems consist of electromechanically actuated elements in dimensions of few nanometers. Consider a typical NEMS actuator made of a movable conducting nanowire suspending over a fixed conductive substrate. By applying a DC potential difference among components, the nanowire deflects towards the substrate due to the presence of the Coulomb attraction. At a critical voltage, which is known as the pull-in voltage, the actuator becomes unstable and adheres to the substrate. Determining the stable actuating range and the pull-in threshold of the system are important issues in designing and fabricating a trustworthy sensors and actuator [1-16].

With the decrease in dimensions to the nano scale, the behaviour of ultra-small systems is influenced by small scale interactions. Regarding the small-scale interactions, the Casimir force (i.e. the vacuum fluctuations), becomes approximate or even dominant if the distance between interacting bodies is larger than a few nanometers and smaller than a few micrometers. In the case of NEMS devices, the Casimir attraction can strongly interfere with the pull-in instability of the systems [17-21]. Furthermore, the Casimir force can induce undesired adhesion in freestanding nanosystems during the fabrication procedures. In this regard, the Casimir force is crucial for modelling the stability of the actuators fabricated from nanowires. It should be mentioned that the geometry of the interacting surfaces plays an important role in determining the strength of the Casimir attraction. An over simple method for approximating the Casimir interaction among non-planar geometries is the proximity force approximation (PFA).

According to the PFA, any complex configuration of interacting surfaces can be treated as a sum of infinitesimal parallel plates [20-22]. Unfortunately, the PFA provides acceptable results only for interacting bodies in very close proximity and hence it is not valid for real objects with considerable separation distances. In this case, the path-integral approach can be employed as a precise method for determining the Casimir attraction. This method was successfully applied by researchers to calculate the Casimir force between non-planar structures, e.g. spheres, sphere-plane and cylinder-plate geometries [21-23].
It should be mentioned that a very limited attention has been devoted to investigate the instability of nanosactuators fabricated from elements with circular cross-sections such as nanowires and nanotubes. Indeed, all previous research in this area has dedicated to the actuators with planar or rectangular geometries. In this regard, present study is allocated to model the influence of the Casimir force on the electromechanical stability of NEMS actuator fabricated from the conductive cylindrical nanowire. The Euler-Bernoulli continuum beam theory is applied to obtain the governing equations of the nanoactuator. To solve the governing equation, three different approaches including the modified variation iteration method (MVIM), the generalized differential quadrature (GDQ) and a lumped parameter model (LPM) solution, are employed.

2. Theoretical Model

Fig. 1 presents a typical NEMS actuator made of nanowire with a circular cross-section which is suspended over the ground plane. The length and the radius of the nanowire are L and R, respectively. The initial gap between the nanowire and the plane is D.

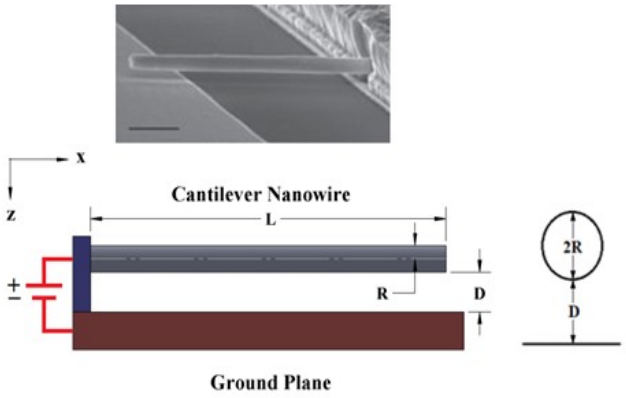

Fig.1. Scanning electron microscopic image and the schematic representation of the nanostructure.

2.1 The vacuum fluctuations

The effect of vacuum fluctuations is expressed in terms of the Casimir force for sufficiently large distances. In most real NEMS applications, the distance between interacting components is large enough. A reliable method for approximating the Casimir force in engineering cases (large distances) is the path integral approach. The path integral approach employs a trace formula for the density of states and determining the Casimir energy. The total electromagnetic Casimir energy is the sum of energies of the Dirichlet and Neumann modes. In the case of large distances, the Dirichlet mode is dominant and thus the Neumann mode may be neglected. In the present study we develop practical mathematical models by assuming the large distance approximation. Considering a cylinder-plate with a large distance, the asymptotic expression of the Casimir energy for the Dirichlet (E^D) mode is evaluated as follows [20, 21]:

$$E^D = -\frac{\overline{h}cL}{16\pi D^2 \ln(\frac{D}{R})} \tag{1}$$

Where $\overline{h}$ =1.054×10^{-34} J.s is the reduced Planck's constant and c=2.998×10^8 m/s is the light speed.
Considering the deflection of the nanowire, w, the Casimir force per unit length can be obtained via differentiating the Casimir energy as:

$$f_{cas} = \frac{dE^D}{dD} = \frac{\overline{h}c}{16\pi(D-w)^3 \ln^2(\frac{D-w}{R})}\left[1+\ln(\frac{D-w}{R})\right] \tag{2}$$

To derive Eq. (2), note that by applying the external voltage on the system, the nanowire will deflect toward the ground level to reduce the in between gap from D to D - w.

2.2 Electrostatic attraction

The electrostatic energy per unit of length of the nanowire can be determined by [24]

$$E_{elec} = \frac{1}{2}C(D)V^2 = \frac{\pi\varepsilon_0 V^2}{\operatorname{arccosh}(1+\frac{D}{R})} \tag{3}$$

Where ε_0 is the permittivity of the vacuum. Now by considering the deflection of the nanowire and by replacing D with D - w in relation (3), the electrostatic force per unit of length, f_{elec}, can be obtained from (3) as:

$$f_{elec} = \frac{dE_{elec}}{dD} = \frac{\pi\varepsilon_0 V^2}{\sqrt{D(D+2R)}\operatorname{arccosh}^2(1+\frac{D}{R})} \tag{4}$$

Where V is the applied voltage.

It is worth noting that the radius of the wire (R) is much smaller than the distance between the nanowire and the ground, D, i.e. $R << D$. Therefore, the electrical force can be approximated as:

$$f_{elec} \approx \frac{\pi\varepsilon_0 V^2}{(D-w)\operatorname{arccosh}^2(\frac{D-w}{R})} = \frac{\pi\varepsilon_0 V^2}{D(1-\frac{w}{D})\times\left[\ln\left(\frac{2D}{R}(1-\frac{w}{D})\right)\right]^2} \tag{5}$$

2.3 Strain energy

According to the continuum theory, the strain energy density of a continuum $\tilde{U}$ can be written as:

$$\tilde{U} = \frac{1}{2}\sigma_{ij}\varepsilon_{ij}, \qquad i,j = 1,2,3, \tag{6}$$

Where the variables σ_{ij} and ε_{ij} are the stress and strain tensor, respectively, and are defined by the following relations:

$$\sigma_{ij} = \lambda\varepsilon_{mm}\delta_{ij} + 2\mu\varepsilon_{ij}, \tag{7-a}$$

$$\varepsilon_{ij} = \frac{1}{2}((\nabla\vec{u})_{ij} + (\nabla\vec{u})^T_{ij}), \tag{7-b}$$

Where λ, μ and $\vec{u}$ are the Lamé constant, shear modulus and the displacement vectors, respectively. Now, by using the Euler-Bernoulli beam model for a nanowire, the displacement field can be expressed as [25]

$$u_1 = -z\frac{\partial w(X)}{\partial X},\ u_2 = 0,\ u_3 = w(X). \tag{8}$$

Considering a small deformation, substituting relation (8) into Eq. (7-a) and using Eq. (6), the strain energy density can be defined as:

$$\begin{aligned} U_{elas} &= \frac{1}{2}\int_0^L\int_A \sigma_{ij}\varepsilon_{ij}\,dA\,dX = \frac{1}{2}\int_0^L\int_A E_{eff}Z^2\left(\frac{\partial^2 w}{\partial X^2}\right)dA\,dX \\ &= \frac{1}{2}E_{eff}I\int_0^L\left(\frac{\partial^2 w}{\partial X^2}\right)^2 dX. \end{aligned} \tag{9}$$

In the above-mentioned relation, $E_{eff}I$, X and A are the effective flexural rigidity of the nanowire (E_{eff} is the effective Young's modulus), the distance from the clamped end and the cross-sectional area of the nanowire,

respectively.

2.4 Governing equations

According to the minimum energy principle, the equilibrium is achieved when the free energy (Π) reaches a minimum value:

$$\delta\Pi = \delta(U_{elas} - W_{cas} - W_{elec}) = 0 \tag{10}$$

Where W_{elec} and W_{cas} is the work done by the electrical and Casimir forces. Therefore, the differential equations of the system is obtained as:

$$\begin{aligned}\delta\Pi &= \delta\left\{\frac{1}{2}\int_0^L E_{eff} I \left(\frac{d^2w}{dX^2}\right)^2 dX - \int_0^L\int_0^w f_{cas}\, dw dX - \int_0^L\int_0^w f_{elec}\, dw dX\right\} \\ &= E_{eff} I \frac{d^2w}{dX^2}\delta\frac{dw}{dX}\bigg|_0^L - E_{eff} I \frac{d^3w}{dX^3}\delta w\bigg|_0^L \\ &+ \int_0^L \left[E_{eff} I \frac{d^4w}{dX^4} - f_{cas} - f_{elec}\right]\delta w dX = 0\end{aligned} \tag{11}$$

And the boundary conditions are obtained as:

$$w(0) = \frac{dw}{dX}(0) = \frac{d^2w}{dX^2}(L) = \frac{d^3w}{dX^3}(L) = 0 \tag{12}$$

Substituting Eq. (12) in Eq. (11), the governing equation of the nanostructure can be obtained as:

$$E_{eff} I \frac{d^4w}{\partial X^4} = f_{cas} + f_{elec}, \tag{13-a}$$

$$w(0) = \frac{dw}{dX}(0) = \frac{d^2w}{dX^2}(L) = \frac{d^3w}{dX^3}(L) = 0. \tag{13-b}$$

By substituting relations (2) and (5) into Eq. (13-a), the dimensionless equation for the actuator is derived as:

$$\begin{aligned}\frac{d^4\hat{w}}{dx^4} &= \frac{\gamma}{(1-\hat{w})^3 \ln\left(\frac{k}{2}(1-\hat{w})\right)} + \frac{\gamma}{2(1-\hat{w})^3 \ln^2\left(\frac{k}{2}(1-\hat{w})\right)} \\ &+ \frac{\beta}{2(1-\hat{w})\ln^2(k(1-\hat{w}))}.\end{aligned} \tag{14-a}$$

$$\hat{w}(0) = \frac{d\hat{w}}{dx}(0) = \frac{d^2\hat{w}}{dx^2}(1) = \frac{d^3\hat{w}}{dx^3}(1) = 0. \tag{14-b}$$

where the dimensionless parameters is defined as:

$$x = \frac{X}{L}, \tag{15-a}$$

$$\hat{w} = \frac{w}{D}, \tag{15-b}$$

$$k = \frac{2D}{R}, \tag{15-c}$$

$$\gamma = \frac{\bar{h}cL^4}{8\pi E_{eff} ID^4}, \tag{15-d}$$

$$\beta = \frac{2\varepsilon_0 \pi V^2 L^4}{E_{eff} I D^2}. \tag{15-e}$$

3. Solution methods

To solve the governing equation, we apply three different approaches.

3.1 Modified Variational Iteration Method (MVIM)

Based on MVIM, the solution to differential equations can be approximated with possible unknowns. The details of the method in solving NEMS problem can be found in [25]. To employ MVIM, Eq. (14-a) is transformed by Taylor expansion to:

$$\frac{d^4 \hat{w}}{dx^4} = \sum_{j=0}^{\infty} a_j [\hat{w}(x)]^j. \tag{16}$$

By applying MVIM, Eq. (16) is reduced to a set of recursive integral equations as:

$$\begin{aligned} \hat{w}_{n+1}(x) &= \frac{c_1}{2} x^2 + \frac{1}{2}\int_0^x (x-\tau)^2 u_n(\tau) d\tau, \\ u_{n+1}(x) &= c_2 + a_0 x + \int_0^x \left\{ \sum_{j=1}^{\infty} a_j [\hat{w}(s)]^j \right\} ds. \end{aligned} \tag{17}$$

With the following initial conditions:

$$\begin{aligned} &\hat{w}_0(x) = 0, \quad u_0(x) = 0, \\ &\hat{w}_0''(0) = c_1, \quad \hat{w}_0'''(0) = c_2 \end{aligned} \tag{18}$$

Finally, the solution of the governing equation is obtained as:

$$\begin{aligned} \hat{w} = {} & \frac{1}{\ln^5(\frac{k}{2})\ln^5(k)} \Big[\frac{1}{2!} c_1 \ln^5(\frac{k}{2})\ln^5(k) x^2 + \frac{1}{3!} c_2 \ln^5(\frac{k}{2})\ln^5(k) x^3 \\ & + \frac{1}{4!}(0.5\beta \ln^5(\frac{k}{2})\ln^3(k) + 0.5\gamma \ln^3(\frac{k}{2})\ln^5(k) + \gamma \ln^4(\frac{k}{2})\ln^5(k)) x^4 \\ & + \frac{1}{6!} c_1 (1.5\beta \ln^5(\frac{k}{2})\ln^2(k) + 0.75\beta \ln^5(\frac{k}{2})\ln^3(k) + 1.5\gamma \ln^2(\frac{k}{2})\ln^5(k) \\ & + 3.75\gamma \ln^3(\frac{k}{2})\ln^5(k) + 4.5\gamma \ln^4(\frac{k}{2})\ln^5(k)) x^6 + \ldots \Big] \end{aligned} \tag{19}$$

The unknown parameters c_1 and c_2 are obtained using the natural boundary conditions (Eq. (18)).

3.2 Generalized differential quadrature (GDQ) method

To solve the governing equation of the system by GDQ, the nanowire is discretized into N-1 elements separated by N nodes. In the GDQ method the r^{th} order derivatives of function f(x) are defined as [26]

$$\left. \frac{\partial^r f}{\partial x^r} \right|_{x=x_i} = \sum_{j=1}^{N} A^{(r)}_{ij} f(x_j), \tag{20}$$

Where the weighed coefficient of derivatives are defined as:

$$A_{ij}^{1}=\frac{M(x_i)}{(x_i-x_j)(M_{x_i})}\ (\mathrm{i,j}=1,2,...,N;\mathrm{i}\neq j),$$

$$A_{ij}^{(r)}=\begin{cases} r\left[A_{ij}^{(r-1)}A_{ij}^{(r)}-\dfrac{A_{ij}^{(r-1)}}{x_i-x_j}\right],\mathrm{i}\neq j \\ -\sum_{j=1}^{N}A_{ij},\mathrm{i}=j \end{cases},\qquad (\mathrm{i,j}=1,2,...,N;2\le r\le N-1) \tag{21}$$

where

$$M(x_i)=\prod_{j=1;\mathrm{j}\neq i}^{N}(x_i-x_j).$$

The sample points of discrete domain are obtained from the Chebyshev–Gauss–Lobatto as:

$$x_i=\frac{L}{2}(1-\cos\frac{i-1}{N-1}\pi),\qquad i=1,2,3,...,N \tag{22}$$

By using Eqs. (21) and (14), the discretized governing equation of system obtained as:

$$\sum_{j=1}^{N}A_{ij}^{(4)}\hat{w}_j=\frac{\beta}{2(1-\hat{w}_i)\ln^2(k(1-\hat{w}_i))}+\frac{\gamma}{(1-\hat{w}_i)^3\ln\left(\frac{k}{2}(1-\hat{w}_i)\right)}+\frac{\gamma}{2(1-\hat{w}_i)^3\ln^2\left(\frac{k}{2}(1-\hat{w}_i)\right)}, \tag{23}$$

Where the boundary conditions are:

$$\hat{w}_1=0,\quad \sum_{j=1}^{N}A_{1j}^{(1)}\hat{w}_j=0,\quad \sum_{j=1}^{N}A_{1j}^{(2)}\hat{w}_j=0,\quad \sum_{j=1}^{N}A_{Nj}^{(3)}\hat{w}_j=0. \tag{24}$$

By numerically solving the algebraic system of equations, the nodal deflections of the nanowire is computed.

3.3 Lumped Parameter Model (LPM)

To develop an appropriate lumped parameter model, the elastic response of the nanowire is modeled by a linear spring with a stiffness of $8E_{eff}I/L^3$ as shown in Fig. 2. This model assumes the uniform Casimir forces along the length of the nanowire.

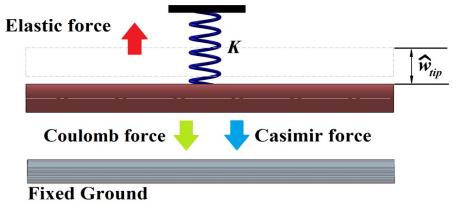

Fig.2. Schematic configuration of the lumped parameter models for a nanoactuator.

Considering the Eq. (14-a), the governing equations of the lumped parameter model for the wire are obtained as:

$$8\hat{w}_{tip}=\frac{\beta}{2(1-\hat{w}_{tip})\ln^2(k(1-\hat{w}_{tip}))}+\frac{\gamma}{(1-\hat{w}_{tip})^3}\frac{1}{\ln\left(\frac{k}{2}(1-\hat{w}_{tip})\right)}+\frac{\gamma}{2(1-\hat{w}_{tip})^3\ln^2\left(\frac{k}{2}(1-\hat{w}_{tip})\right)} \tag{25}$$

4. Results and Discussion

Fig. 3a shows the variation of centerline deflection of nanowire ($\hat{w}$) as a function of the dimensionless applied voltage while neglecting the effect of vacuum fluctuations. Fig. 3b depicts the variation of the centerline deflection considering the Casimir force ($\gamma = 3$). As shown above, increasing the dimensionless voltage (β) leads to an increase in the nanowire deflection. When the electrostatic attraction overcomes the elastic resistance of the nanowire, instability occurs and the actuator adheres to the ground. Note that the design of the NEMS actuator is limited by this instability. Comparing Figs. 4a and 6b demonstrate that due to the presence of the Casimir force, the dimensionless instability voltage of the nanoactuator is reduced from 123.71 to 63.35. Moreover, Fig. 3b shows that the nanowire has an initial deflection due to the presence of vacuum fluctuations even when no electrostatic force is applied.

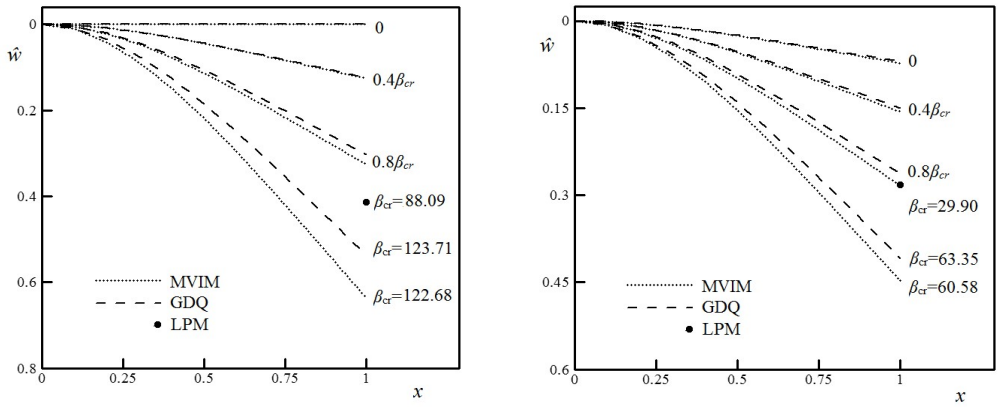

(a) (b)

Fig.3. Displacement variation of the nanowire for different values of β and k = 200 (a) by neglecting the Casimir force (b) and considering Casimir force (γ = 2).

The effect of vacuum fluctuations on the stability behavior of the nanowire is presented in Fig.4 regarding different solution methods. This figure shows the variation of the nanowire tip displacement ($\hat{w}_{tip}$) as a function of the dimensionless voltage (β) for different values and for the Casimir attraction parameter (γ). Moreover, the variation of $\hat{w}_{tip}$ as a function of β for different k values and a constant Casimir force parameter ($\gamma = 1.5$) is shown in Figs. 5. As can be seen, for any given β, where $\beta \leq \beta_{cr}$, one can find solutions for $\hat{w}_{tip}$. However, when $\beta > \beta_{cr}$, no solution exists for $\hat{w}_{tip}$. This means that the instability occurs and the nanowire adheres to the ground. The values of β_{cr} and the corresponding nanowire critical tip deflection, $\hat{w}_{cr}$, can be determined from the β-$\hat{w}_{tip}$ curves (Figs. 4 and 5). At the onset of instability, the slope of the curves approaches infinity ($d\hat{w}_{tip}/d\beta=\infty$). This reveals the possibility of further increase in the deflection even without any increase in the force(s). Fig. 4 reveals that an increase in the Casimir parameter γ reduces the instability voltage (β_{cr}) and the maximum tip displacement ($\hat{w}_{tip}$) of the nanowire. Similar trend is seen in Fig. 5, where increase in k value results in an upward trend in β_{cr} and the maximum value of $\hat{w}_{tip}$.

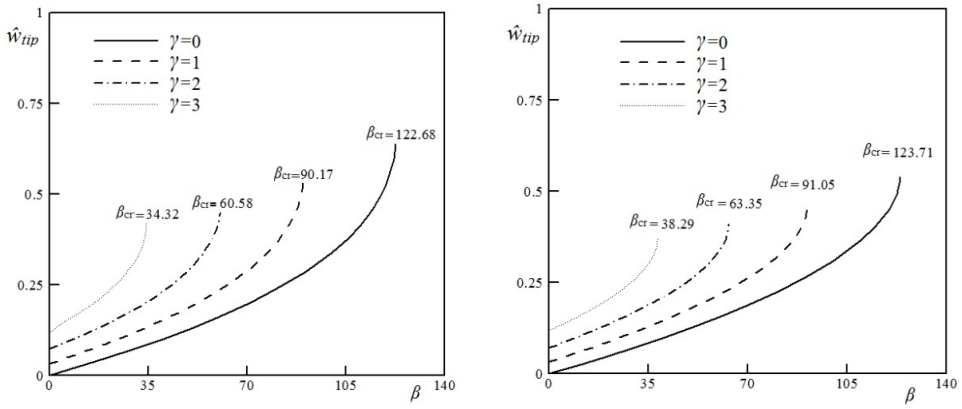

(a) (b)

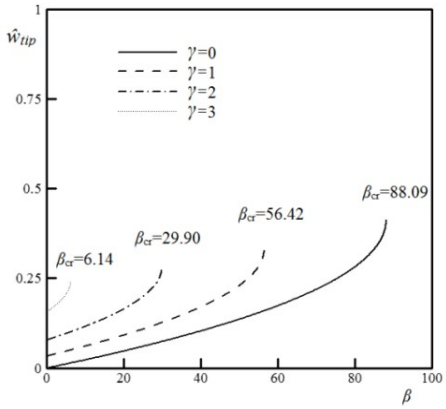

(c)

Fig.4. The variation of the tip displacement of the nanowire versus β for k = 200 using γ = 0, γ = 1, γ = 2 and γ = 3, (a) MVIM, (b) GDQ, (c) LPM.

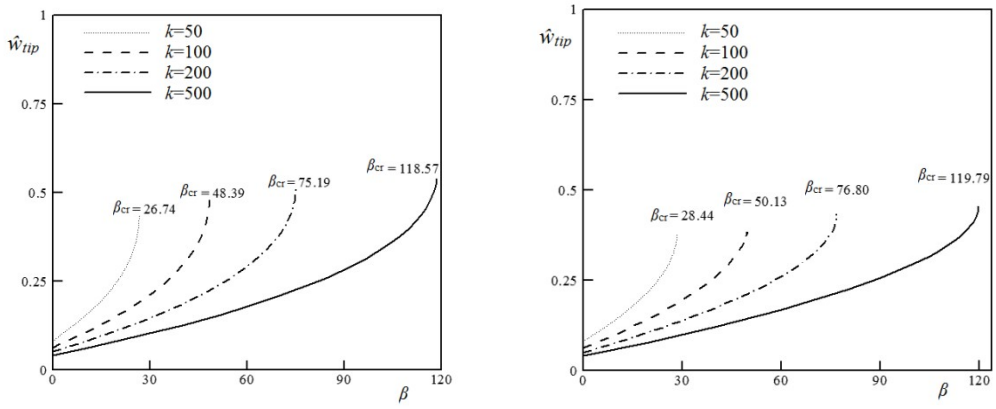

(a) (b)

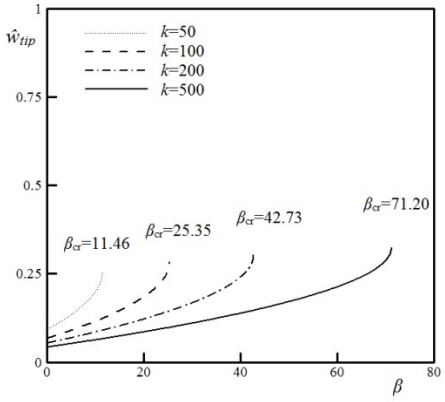

(c)

Fig.5. The variation of β versus the tip displacement of the nanowire for γ = 1.5 using k = 50, k = 100, k = 200 and k = 500, (a) MVIM, (b) GDQ, (c) LPM.

For a freestanding actuator (no Coulomb attraction), when the vacuum fluctuations (γ) exceed the critical value (γ_{cr}), no solution exists for the nanowire deflection and thus nanowire adheres the substrate. The maximum permissible length of the nanowire L_{max}, to prevent the adherence is very important in design and fabrication of nanoactuators [18-20]. The value of L_{max} can be determined by computing γ_{cr} (considering β=0 and solving Eq. (14)), and then substituting γ_{cr} into the definition of γ (Eq. (15-d)). The variation of L_{max} for typical freestanding nanoactuator as a function of the wire diameter and initial gaps is illustrated in Fig.6. For the sake of comparison, two small-scale force regime including Casimir (Eq. (2)) and vdW (Eq. (26)) are considered for computing L_{max}. The

typical nanoactuator is made of carbon nanowires with the diameter of 100 nm and E=1TPa. As can be seen in Fig. 6, for a small distance (D=100 nm), the L_{max} values predicted by Casimir regime assumption is close to that of vdW regime assumption. However, at larger gap distances (D=500nm), assuming the Casimir force regime leads to higher values of L_{max} in comparison with the vdW regime.

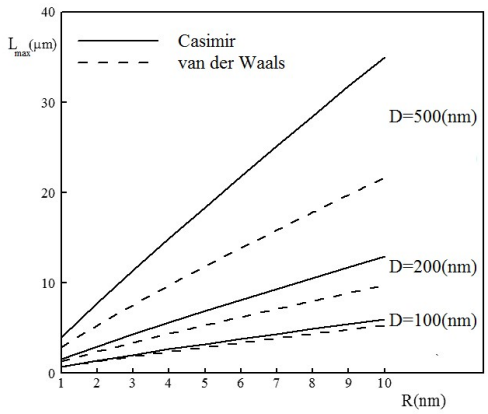

Fig.6. The variation of the nanowire stable length as a function of the wire diameter and the initial gap using the Casimir and vdW forces.

5. Conclusions

The effect of the Casimir force on the electromechanical response of actuators fabricated from cylindrical nanowire was demonstrated. The difference between the Casimir and vdW regimes was illustrated by comparing the forces for typical cylinder-plate geometry. It was found that the Casimir attraction reduces the pull-in voltage and deflection of the actuator. The maximum stable length of freestanding actuator was determined and a good agreement between the GDQ and MVIM solutions was observed. The results show that the LPM found to be beneficial for modeling the behavior of the actuator without any mathematical complexity.

References

[1] Ghalambaz, M., Ghalambaz, M., Edalatifar, M., "Buckling Analysis of Cantilever Nanoactuators Immersed in an Electrolyte: A Close Form Solution Using Duan-Rach Modified Adomian Decomposition Method", Journal of Applied and Computational Mechanics, 1(4), pp. 207-219, 2015.

[2] Mokhtari, J., Farrokhabadi, A., Rach, R., and Abadyan, M., "Theoretical modeling of the effect of Casimir attraction on the electrostatic instability of nanowire-fabricated actuators", Physica E: Low-dimensional Systems and Nanostructures, 68, pp. 149-158, 2015.

[3] Farrokhabadi, A., Mokhtari, J., Rach, R., and Abadyan, M., "Modeling the influence of the Casimir force on the pull-in instability of nanowire-fabricated nanotweezers", International Journal of Modern Physics B, 29, 2, pp. 1450245, 2015.

[4] Farrokhabadi, A., Mokhtari, J., Koochi, A., and Abadyan, M., "A theoretical model for investigating the effect of vacuum fluctuations on the electromechanical stability of nanotweezers", Indian Journal of Physics, 89, 6, pp. 599-609, 2015.

[5] Keivani, M., Gheisari, R., Kanani, A., Abadian, N., Mokhtari, J., Rach, R., and Abadyan, M., "Effect of the centrifugal force on the electromechanical instability of U-shaped and double-sided sensors made of cylindrical nanowires", Journal of the Brazilian Society of Mechanical Sciences and Engineering, 38, 7, pp. 2129-2148, 2016.

[6] Keivani, M., Kanani, A., Mardaneh, M. R., Mokhtari, J., Abadyan, N., and Abadyan, M., "Influence of Accelerating Force on the Electromechanical Instability of Paddle-Type and Double-Sided Sensors Made of Nanowires", International Journal of Applied Mechanics, 8, 1,pp. 1650011, 2016.

[7] Keivani, M., Khorsandi, J., Mokhtari, J., Kanani, A., Abadian, N., and Abadyan, M., "Pull-in instability of paddle-type and double-sided NEMS sensors under the accelerating force", Acta Astronautica, 119, pp.196-206, 2016.

[8] Farjam, N., "Pull-in behavior of a bio-mass sensor based on an electrostatically actuated cantilevered CNT with consideration of rippling effect", Journal of Applied and Computational Mechanics, 1(4), pp. 229-239, 2015.

[9] Keivani, M., Mokhtari, J., Kanani, A., Abadian, N., Rach, R., and Abadyan, M., "A size-dependent model for instability analysis of paddle-type and double-sided NEMS measurement sensors in the presence of centrifugal force", Mechanics of Advanced Materials and Structures, just-accepted, 2016.

[10] Keshtegar, B., Ghaderi, A., El-Shafie, A., "Reliability analysis of nanocomposite beams-reinforced by CNTs under buckling forces using the conjugate HL-RF", Journal of Applied and Computational Mechanics, 2(4), pp. 200-207, 2016.

[11] Keivani, M., Abadian, N., Koochi, A., Mokhtari, J., and Abadyan, M., "A 2-DOF microstructure-dependent model for the coupled torsion/bending instability of rotational nanoscanner", Applied Physics A, 122, 10, pp. 927, 2016.
[12] Sedighi, H. M., Keivani, M., and Abadyan, M., "Modified continuum model for stability analysis of asymmetric FGM double-sided NEMS: corrections due to finite conductivity, surface energy and nonlocal effect", Composites Part B: Engineering, 83, pp. 117-133, 2015.
[13] Keivani, M., Mokhtari, J., Abadian, N., Abbasi, M., Koochi, A., and Abadyan, M., "Analysis of U-shaped NEMS in the Presence of Electrostatic, Casimir, and Centrifugal Forces Using Consistent Couple Stress Theory", Iranian Journal of Science and Technology, Transactions A: Science, just-accepted, pp. 1-12, 2017.
[14] Sedighi, H. M., Daneshmand, F., and Abadyan, M., "Modified model for instability analysis of symmetric FGM double-sided nano-bridge: corrections due to surface layer, finite conductivity and size effect", Composite Structures, 132, pp. 545-557, 2015.
[15] Vakili Tahami, F., Biglari, H., Raminnea, M., "Optimum design of FGX-CNT-reinforced Reddy pipes conveying fluid subjected to moving load", Journal of Applied and Computational Mechanics, 2(4), pp. 243-253, 2016.
[16] Mohsen-Nia, M., Abadian, F., Abadian, N., Dehkordi, K. M., Keivani, M., and Abadyan, M., "Analysis of cantilever NEMS in centrifugal-fluidic systems", International Journal of Modern Physics B, 30, 22, pp. 1650148, 2016.
[17] Koochi, A., Kazemi, A.S., Tadi Beni, Y., Yekrangi, A. and Abadyan, M., "Theoretical study of the effect of Casimir attraction on the pull-in behavior of beam-type NEMS using modified Adomian method", Physica E., 43, 2, pp. 625-632, 2010.
[18] Lin, W. H., and Zhao, Y. P., "Casimir effect on the pull-in parameters of nanometer switches", Microsystem Technologies, 11, pp. 80-85. 2005.
[19] Lin, W. H., and Zhao, Y. P., "Nonlinear behavior for nanoscales electrostatic actuators with Casimir force", Chaos Solitons Fractals, 23, pp. 1777-1785, 2005,
[20] Farrokhabadi, A., Abadian, N., Rach, R., and Abadyan, M., "Theoretical modeling of the Casimir force-induced instability in freestanding nanowires with circular cross-section", Physica E: Low-dimensional Systems and Nanostructures, 63, pp. 67-80, 2014.
[21] Farrokhabadi, A., Abadian, N., Kanjouri, F., and Abadyan, M., "Casimir force-induced instability in freestanding nanotweezers and nanoactuators made of cylindrical nanowires", International Journal of Modern Physics B, 28, 19, pp. 1450129, 2014.
[22] Bordag, M., "The Casimir effect for a sphere and a cylinder in front of plane and corrections to the proximity force theorem", Physical Review D, 73, pp. 125018, 2006,
[23] Emig, T., Jaffe, R.L., Kardar, M. and Scardicchio, A., "Casimir Interaction between a Plate and a Cylinder", Physical review letters, 96, pp. 080403, 2006,
[24] Hayt, W.H., Engineering Electromagnetics. 4th edn., McGraw-Hill, New York, 1981.
[25] Koochi, A., Farrokhabadi, A., and Abadyan, M., "Modeling the size dependent instability of NEMS sensor/actuator made of nano-wire with circular cross-section", Microsystem Technologies, 21, 2, pp. 355-364, 2015.
[26] Shu, C.H., Differential quadrature and its application in engineering, Springer, London, 1999.
[27] Israelachvili, J.N., Intermolecular and Surface Forces, Academic Press, London, 1992.
[28] Ke, C. H., Pugno, N., Peng, B., and Espinosa, H. D., "Experiments and modeling of carbon nanotube-based NEMS devices", Journal of the Mechanics and Physics of Solids, 53, 6, pp. 1314-1333, 2005.
[29] Kashyap, K.T., Patil, R.G. and Bull, R.G., "on Young's modulus of multi-walled carbon nanotubes", Bulletin of Materials Science, 31, 2, pp. 185-187, 2008.